Mesoporous Bifunctional K_2O Catalyst Using Chitosan Template for Biodiesel Production

Nor Badariah Talib[1], *Khairil Juhanni Abd* Karim[1], *Nurrulhidayah* Salamun[1], *Salmiah Jamal Mat* Rosid[2], and *Susilawati* Toemen[1*]

[1]Department of Chemistry, Faculty of Science, Universiti Teknologi Malaysia, 81310 UTM Skudai, Johor, Malaysia
[2]UNISZA Science and Medicine Foundation Centre, Universiti Sultan Zainal Abidin, Besut Campus, 22200 Besut Terengganu, Malaysia

Abstract. Mesoporous metal oxides are highly effective catalysts for biodiesel production due to their large surface area and adjustable pore structures, which enhance mass transfer and catalytic activity. In this study, a mesoporous K_2O catalyst was prepared using chitosan, a natural polymer, as a template. Chitosan was first dissolved in a mild acetic acid solution and mixed with potassium nitrate at an optimized ratio. The mixture was stirred and then added dropwise into a sodium hydroxide solution, inducing the formation of solid spherical beads through chemical bonding. The beads were then dried, and calcined at 700 °C for 2 h. This calcination step removed the organic chitosan, creating a porous structure, while converting potassium compounds into active catalytic species including K_2O, K_2O_2, and $K_2CO_3 \cdot 1.5H_2O$, which also helped maintain the bead morphology. SEM analysis revealed a dense, porous structure, while the catalyst's bifunctional nature was confirmed by a total basicity of 1.346 mmol/g and total acidity of 1.515 mmol/g. The optimised synthesis conditions yielded a maximum biodiesel yield of 95.26%, demonstrating the catalyst's potential for efficient biodiesel production.

1 Introduction

The extensive use of fossil fuels for transportation, energy, and industry contributes to global warming and greenhouse gas emissions. Biodiesel is recognized as a sustainable alternative to diesel due to its similar physicochemical properties [1]. Converting waste cooking oil (WCO) into biodiesel not only ensures energy security but also reduces pollution, protects food safety, and supports sustainable growth. Alkali metals are known for their strong basicity, with potassium-based catalysts offering highly reactive basic sites, particularly effective in transesterification [1,2]. Mesoporous metal oxide (MMO) bead catalysts, with pore sizes ranging from 2 to 50 nm, offer several advantages, including lower metal loading, ease of recovery, and reusability. These can be synthesized using organic templates that decompose during thermal treatment [3]. Designing MMO remains challenging because the high reactivity of metal precursors hinders control over ordered structure formation. Natural

* Corresponding author: susilawatitoemen@utm.my

polymers, such as chitosan, offer a promising and cost-effective template solution due to their metal-binding properties. Using such polymers can overcome the difficulty of directing the assembly of reactive metal precursors. Chitosan, a biopolymer derived from chitin deacetylation, contains hydroxyl and amino groups that strongly bind metal ions, making it ideal for preparing heterogeneous catalysts. These functional groups enable strong interactions with potassium, while gelation in NaOH forms spherical particles through physical crosslinking. Chitosan also facilitates controlled assembly of metal species due to its well-dispersed, naturally spaced amino groups (5.8 mmol/g) [4]. This study aims to synthesize a mesoporous bifunctional K_2O-based catalyst using chitosan via ionic gelation and calcination, and to evaluate its structure, acid-base properties, and performance in WCO transesterification.

2 Materials and Method

2.1 Materials

Potassium nitrate (KNO_3), chitosan (low molecular weight, 75% deacetylated, for the synthesis of K2O-Chitosan were purchased from Sigma-Aldrich. While glacial acetic acid (99%) and sodium hydroxide (NaOH), purchased from Merck and Qrec. For transesterification, methanol, n-hexane, and methyl nonadecanoate (as reactant, solvent, and internal standard) were sourced from Sigma-Aldrich. Waste cooking oil (WCO) was collected from student cafeterias at UTM. Prior to use, WCO was filtered (Whatman Grade 1) and heated to 100 °C to remove moisture.

2.2 Synthesis of mesoporous K_2O-chitosan catalyst

Chitosan beads were prepared via ionic gelation, as described by Sutirman (2020) [5], with modifications for potassium incorporation. Chitosan (4 g) was dissolved in 200 mL of 0.5% (v/v) acetic acid, followed by the addition of 10.01 g KNO_3 (4:1 K:chitosan monomer ratio). The mixture was stirred for 3 h at room temperature and left overnight to remove surface bubbles. The resulting solution was added dropwise to 1 M NaOH under stirring to form spherical beads, which were equilibrated for 5 hours. Beads were washed with distilled water, dried at 60°C overnight, and then calcined at 700°C for 2 hours. Catalyst preparation was optimized by varying the K:chitosan monomer ratio.

2.3 Transesterification reaction

For transesterification, 10 g of oil was heated to 65°C in a 50 mL round-bottom flask for 20 minutes. Then, 0.6 g of catalyst (6 wt%) and 6.6 g of methanol (18:1 methanol-to-oil ratio) were added, and the mixture was refluxed with stirring for 3 hours. Biodiesel was analysed using a GC-FID with a DB-HeavyWAX column (30 m × 0.25 mm × 0.25 μm) and helium as the carrier gas. The oven temperature was programmed as follows: 60 °C (2-minute hold), ramped to 200 °C at 10 °C/min, then to 240 °C at 5 °C/min (7-minute hold). Injector and detector temperatures were set at 250 °C. Samples were diluted with 10,000 ppm internal standard, and 1 μL was injected. The chromatogram was analyzed using GC ChemStation software. Biodiesel purity was determined per EN 14103, and yield was calculated using Equation (1).

$$\text{Yield } (\%) = \left(\frac{weight\ of\ biodiesel}{weight\ of\ raw\ oil}\right) \times \left(\frac{\Sigma peak\ area - IS\ area}{IS\ area} \times \frac{IS\ weight}{weight\ of\ sample} \times 100\right) \quad (1)$$

2.4 Characterization of mesoporous K_2O-chitosan catalyst

The crystal structure of the catalyst was analysed using XRD (Siemens D5000 Crystalloflex with a D/Tex Ultra 250 (H) detector). Ground samples were placed on a 1 mm deep, 10–15 μm diameter glass sample holder. Data were collected over a 2θ range of 20°–80° at a scan rate of 3°/min and analysed using SmartLab Studio II software, then compared to the Inorganic Crystal Structure Database (ICSD). Catalyst basicity was determined via Hammett indicator titration using 0.05 M benzene carboxylic acid in methanol [6]. A 0.1 g sample was suspended in 20 mL methanol, and titrated with the acid after adding phenolphthalein. Basicity (mmol/g) was calculated from the volume of the titrant. Acidity was measured following Lai et al. [7]. A 0.05 g catalyst sample was stirred in 45 mL acetonitrile for 3 h, then titrated with 0.05 M n-butylamine in acetonitrile using phenolphthalein. Acidity (mmol/g) was calculated from the volume of titrant used. Surface morphology and elemental composition were examined using SEM (JEOL JSM-IT300LV) at 30 kV. Samples were platinum-coated by electro-deposition and imaged under a tungsten filament electron beam at a resolution of 5.0 kV.

3 Results and Discussion

3.1 Synthesis and catalytic activity of K_2O–chitosan catalyst towards transesterification of WCO

Fig. 1 illustrates the synthesis pathway of mesoporous bifunctional K_2O-Chitosan catalyst. Chitosan was first dissolved in acetic acid to form a viscous slurry, then mixed with potassium ions, forming complexes via coordination with amine and hydroxyl groups. These complexes stabilised the distribution of potassium within the polymer matrix. The mixture was then dropped into NaOH to induce ionic gelation, forming spherical beads that encapsulated the potassium species. Calcination at 700 °C for 2 h decomposed the polymer, creating porosity and converting potassium to active K_2O and K_2O_2 phases. Simultaneously, CO_2 and H_2O released during decomposition reacted with K_2O to form $K_2CO_3 \cdot 1.5H_2O$, which acted as a structural binder. Strong hydrogen bonding and ionic interactions among K_2O, K_2O_2, and $K_2CO_3 \cdot 1.5H_2O$ maintained the bead structure and stability. In the final catalyst, K_2O and K_2O_2 function as Brønsted bases, while K_2CO_3 provides Lewis acidic sites, enabling the efficient transesterification of high-FFA, high-TAN feedstocks, such as WCO, without requiring pretreatment.

Fig. 2a compares the performance of chitosan, dried K–chitosan, and K_2O–chitosan. Chitosan alone yielded 15.19% biodiesel, which increased to 41.14% after potassium incorporation (4:1 K:chitosan, 0.5 v/v% acetic acid), likely due to the catalytic activity of potassium species [2]. Calcination at 700 °C for 2 h further increased the yield to 95.17% and the purity from 74.99% to 100%, indicating the formation of a metal oxide and a mesoporous structure that enhanced catalytic performance.

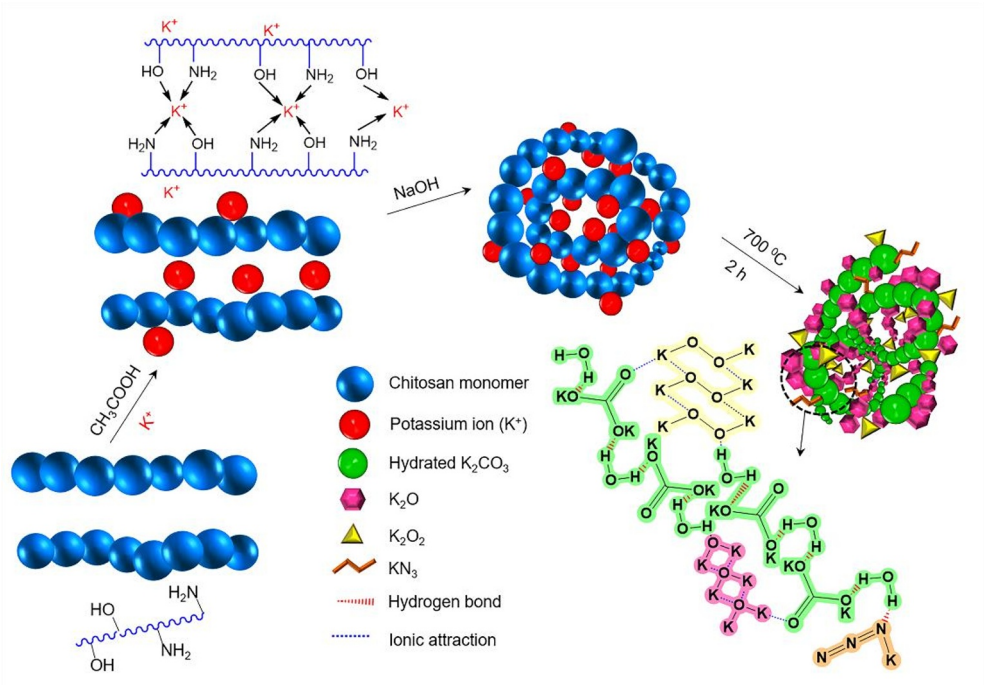

Fig. 1. Proposed synthesis pathway of mesoporous bifunctional K_2O-Chitosan catalyst.

The potassium-to-chitosan monomer ratio was optimised by varying it from 3:1 to 5:1, while keeping the acetic acid concentration (0.5 v/v%) and calcination time (2 h at 700 °C) constant. Increasing the potassium ratio improved the biodiesel yield from 77.20% (3:1) to a peak of 95.17% (4:1) and purity to 100%, as shown in Fig. 2b. However, further increasing the ratio to 5:1 reduced the yield to 88.96%. This is attributed to enhanced basicity resulting from increased K_2O formation; however, excess potassium disrupted the template structure [8] and promoted soap formation via triglyceride saponification, thereby reducing the yield [9].

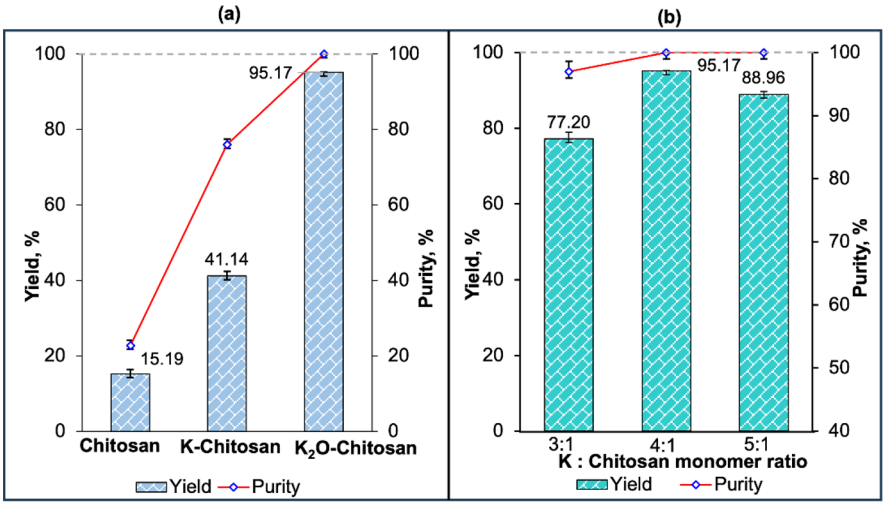

Fig. 2. (a) Catalytic activity of chitosan bead, dried K-Chitosan bead and K_2O-Chitosan bead catalysts and (b) optimization of K:Chitosan monomer ratio towards transesterification of WCO.

3.2 X-Ray diffraction analysis

Fig. 3 presents the XRD patterns of mesoporous bifunctional K_2O-Chitosan catalysts with varying potassium loadings, matched with the ICSD database. No peaks for KNO_3 were observed, confirming its complete decomposition at 700 °C. All samples show cubic K_2O peaks at 2θ = 32.2°, 32.8°, 37.8°, 51.0° and 55.1° (ICSD 00-027-0431). There are also hexagonal K_2O peaks that emerged at 2θ = 29.1°, 29.5°, 31.8°, 36.6°, 37.9°, 40.6°, 43.8°, and 45.0 (ICSD 00-026-1327), likely due to solid-phase transitions induced by the increased potassium concentration, as supported by Guder and Dalgic [10].

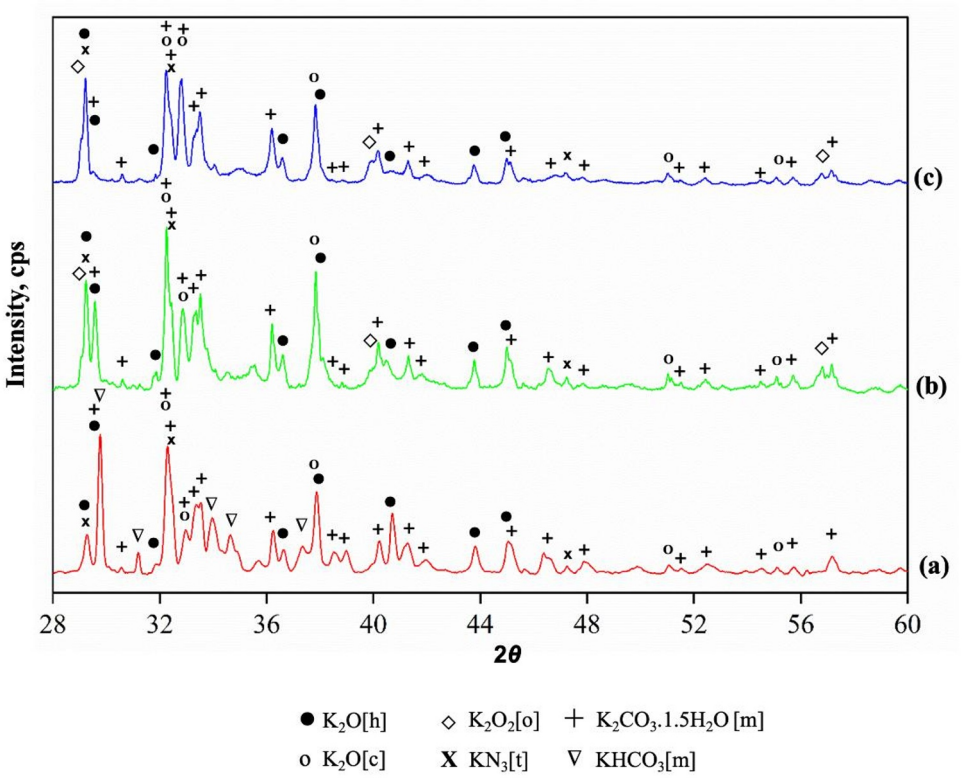

Fig. 3. XRD pattern of K2O-Chitosan at potassium to chitosan loading of (a) 3:1, (b) 4:1, and (c) 5:1 calcined at 700ºC for 2 h.

Orthorhombic K_2O_2 (ICSD 00-032-0827) peaks at 2θ = 29.0°, 39.8°, and 57.0° were also detected at higher loadings (4 and 5), indicating oxidation of K_2O. This phase was absent at lower loadings, where K_2O remains more stable. Despite its lower stability, the K_2O_2 phase may be stabilized by structural binders. Notably, monoclinic $K_2CO_3 \cdot 1.5H_2O$ (ICSD 01-073-0470) was observed across all samples, formed from the reaction of K_2O with CO_2 and the moisture released during chitosan decomposition, which contributed to the structural integrity. At low potassium loading (ratio 3), monoclinic $KHCO_3$ (ICSD 01-082-1447) was observed at 2θ = 29.9°, 31.2°, 34.0°, 34.6°, and 37.5°, suggesting excess CO_2 further carbonated the hydrated K_2CO_3. As previously discussed, hydrated K_2CO_3 acts as a binder that is critical for maintaining structural integrity; its absence compromises mechanical strength. The non-optimized potassium ratios (3 and 5) clearly affected the binder amount, as shown in Fig. 3. This, in turn, influenced the number of active sites since the binder plays a crucial role as an adhesive for these sites. The notable reduction in K_2O peak intensity

supports this observation, which explains the decreased catalytic performance illustrated in Fig. 2b. Peaks for tetragonal KN_3 (ICSD 00-048-1276) at 2θ = 29.1°, 32.4° and 47.2° confirmed interactions between chitosan's amine groups and potassium ions.

3.3 Scanning electron microscopy (SEM)

Fig. 4 shows the morphology of K_2O–Chitosan (4:1 K ratio, 0.5 v/v% acetic acid, calcined at 700 °C for 2 h) at various magnifications. As shown in Fig. 4a, porosity is formed by loosely connected, plate-like strips that resemble a flower-like network. Further magnification at 300k revealed that each plate is composed of closely packed spherical particles, with an average diameter of 15.21 nm, confirming its mesoporous nature. During calcination, chitosan decomposes, releasing CO_2 and H_2O, which can react with potassium oxide to form $K_2CO_3 \cdot 1.5H_2O$, as confirmed by XRD in Fig. 3. This hydrated phase forms a loose network that acts as a binder, maintaining catalyst structure after template decomposition.

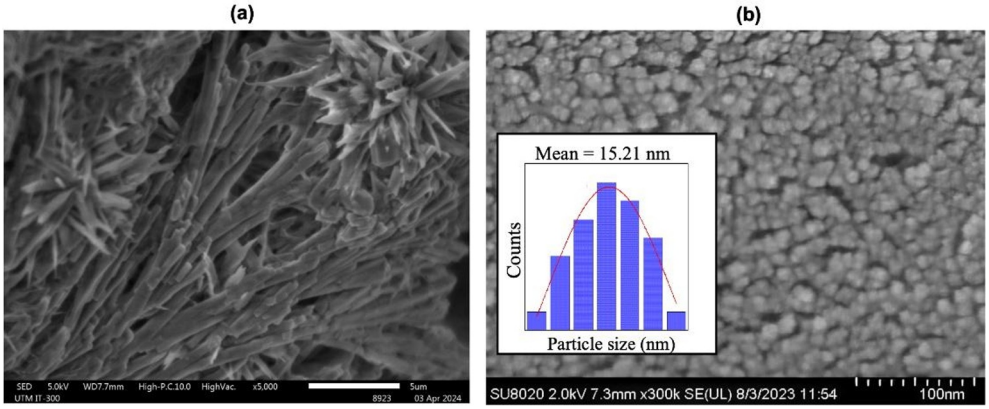

Fig. 4. (a) SEM micrograph at 5000 magnification, (b) FESEM micrograph at 300.000 magnification, and its particle size distribution of K_2O-Chitosan prepared at 4:1 potassium to chitosan ratio, 0.5 v/v% acetic acid, 2 h calcination time at 700 °C.

3.4 Total basicity and acidity using Hammett analysis

The total basicity and acidity of K2O-Chitosan catalysts when synthesized at different potassium ratio are depicted in Table 1. Increasing the potassium molar ratio from 3 to 4 significantly enhanced both the catalyst's basicity (0.458 to 1.346 mmol/g) and acidity (0.630 to 1.515 mmol/g), likely due to the increased presence of K_2O and K_2O_2 species, as confirmed by XRD. Stronger basicity, linked to denser basic sites, is crucial for catalytic activity, as shown in Fig. 2b. However, further increase to 5 reduced both basicity (0.629 mmol/g) and acidity (0.867 mmol/g) due to diminished K_2O content. The carbonyl carbon in $K_2CO_3 \cdot 1.5H_2O$, besides acting as a binder, also contributes to Lewis acidity, confirming the bifunctional nature of the 4:1 K_2O-chitosan catalyst. The binder not only plays a critical role in maintaining structural integrity and synergizing with the active sites, but its reduced amount also negatively affected the acidity. This reduction is clearly evident in the XRD results, which show a decrease in binder intensity that is reflected in the catalyst's basicity and acidity, ultimately impacting the biodiesel yield, as shown in Fig. 2b. Overall, the catalyst properties were strongly influenced by the synthesis conditions, directly affecting its catalytic activity.

Table 1. Total basicity, total acidity and biodiesel yield of K2O-Chitosan catalysts synthesized at different parameters.

K_2O-Chitosan	Total basicity, mmol/g	Total acidity, mmol/g
3:1 0.5 2 h	0.458	0.630
4:1 0.5 2 h	1.346	1.515
5:1 0.5 2 h	0.629	0.867

4 Conclusion

The mesoporous bifunctional K_2O-Chitosan bead catalyst was successfully synthesised using ionic gelation and potassium complexation, with varying potassium-to-chitosan monomer ratios (3:1 to 5:1). XRD analysis identified the presence of K_2O and K_2O_2 phases, which acted as Brønsted bases, while hydrated K_2CO_3 played a crucial role as Lewis acid and a binder, maintaining the bead shape of the catalyst and contributing to its structural stability. The catalyst was demonstrated to possess bifunctional properties through Hammett analysis, exhibiting a total basicity of 1.346 mmol/g and a total acidity of 1.515 mmol/g. SEM study revealed that the catalyst possessed a highly porous structure composed of loosely connected plate strips forming a network. While this study did not explore catalyst regeneration and reusability, these aspects present valuable opportunities for future research aimed at enhancing durability and assessing long-term catalytic performance.

Acknowledgments

This work was supported by the Universiti Teknologi Malaysia through UTM Fundamental Research Grant (UTMFR)(Q.J130000.3854.22H42) and financial support (Nor Badariah Talib) from Yayasan Sultan Iskandar Johor.

References

1. Roy, T., Agarwal, A. K., Sharma, Y. C. (2021). A Cleaner Route of Biodiesel Production from Waste Frying Oil using Novel Potassium Tin Oxide Catalyst: A Smart Liquid-Waste Management. Waste Management. 135: 243-255.
2. Kosawatthanakun, S., Pansakdanon, C., Sosa, N., Chanlek, N., Roessner, S., Prayoonpokarach, S., Wittayakun, J. (2022). Comparative Properties Of K/Nax And K/Nay from Ultrasound-Assisted Impregnation and Performance in Transesterification of Palm Oil. ACS Omega. 7:9130-9141.
3. Sathyan, A., Deng, L., Loman, T., Palmans, A. R. A. (2023). Bioorthogonal Catalysis in Complex Meida: Consequences of Using Polymeric Scaffold Materials on Catalyst Stability and Activity. Catalysis Today. 418: 114116.
4. El Kadib, A. (2015). Chitosan as a sustainable organocatalyst: a concise overview. ChemSusChem, 8(2), 217-244.
5. Sutirman, Z. A., Rahim, E. A., Sanagi, M. M., Abd Karim, K. J., & Ibrahim, W. A. W. (2020). New Efficient Chitosan derivative for Cu (II) Ions Removal: Characterization and Adsorption Performance. Int. J. Biol.l Macromol., 153, 513-522.
6. Takase, M., Bryant, I. M., Essandoh, P. K., Amankwa, A. E. K. (2023). A Comparative Study on performance of KOH and 32%KOH/ZrO2-7 Catalyst for Biodiesel via Transesterification of Waste Adansonia Digitata Oil. Green Technol. Sustain. 1,100004.

7. Lai, F., Yan, F., Wang, P., Wang, S., Li, S., Zhang, Z.(2020). Highly Efficient Conversion of Cellulose into 5-hydroxymethylfurfural using Temperature-responsive ChnH5-nCeW12O40 (n=1-5) Catalyst. Chem. Eng. J., 396, 125282.
8. Azancot, L., Bobadilla, L. F., Centeno, M. A., Odriozola, J. A. (2021). Effect of Potassium Loading on Basic Properties of Ni/Mgal2O4 Catalyst for CO2 Reforming of Methane. Journal of CO2 Utilization. 52 : 101681
9. Baydir, E., Aras, O. (2022). Increasing Biodiesel Production Yield in Narrow Channel Tubular Reactors. Chemical Engineering and Processing - Process Intensification. 170: 108719
10. Guder, V., & Senturk Dalgic, S. (2017). Thermodynamic Properties of Potassium Oxide (K_2O) Nanoparticles by Molecular Dynamics Simulations. Acta Phys. Polonica A, 131(3), 490-494.